

1 Ionospheric response to the 2009 sudden stratospheric warming over the
2 equatorial, low- and mid-latitudes in the South American sector

3

4 Fagundes¹ PR, Goncharenko² LP, de Abreu¹ AJ, Gende³ M, de Jesus¹ R,
5 Pezzopane⁴ M, Venkatesh¹ K, Coster² AJ and Pillat¹ VG

6

7 1- Física e Astronomia, Universidade do Vale do Paraíba (UNIVAP), São José
8 dos Campos, São Paulo, Brazil.

9

10 2- MIT Haystack Observatory, Massachusetts Institute of Technology,
11 Westford, Massachusetts, USA.

12

13 3- Facultad de Ciencias Astronomicas y Geofisicas, Universidad Nacional de
14 La Plata, La Plata, Argentina.

15

16 4- Istituto Nazionale di Geofisica e Vulcanologia, 00143 Rome, Italy.

17

18 **Abstract**

19 The present study investigates the consequences of vertical coupling from lower to
20 the upper atmosphere in the equatorial and low-latitude ionosphere in Southern
21 Hemisphere during a major SSW event, which took place during January-February
22 2009 in the Northern Hemisphere. Using seventeen ground-based dual-frequency
23 GPS stations and two ionosonde stations spanning from latitude 2.8°N to 53.8°S
24 and from longitude 36.7°W to 67.8°W over the South American sector, it has been

25 observed that the ionosphere was significantly disturbed by the SSW event from
26 Equator to the mid-latitudes. Using one GPS station located at Rio Grande (53.8°S,
27 67.8°W, mid-latitude-South America sector) it is reported for the first time that the
28 mid-latitude in southern hemisphere was disturbed by the SSW event in the
29 Northern hemisphere. For instance, during DOY 26 and 27 at 14:00 UT the TEC
30 were twice larger than those observed during averaged quiet days. The VTEC at
31 all 17 GPS and two ionosonde stations show significant deviations lasting for
32 several days after the SSW temperature peak.

33

34 **1. Introduction**

35 The equatorial and low-latitude ionosphere/thermosphere system is
36 predominantly disturbed by waves (MSTIDs, tides, and planetary waves), which
37 are generated in the lower atmosphere or in-situ, as well as electric fields and TIDs
38 produced by geomagnetic storm and UV, EUV, and X-ray solar radiation. For many
39 years, it was thought that, during geomagnetic quiet conditions, the equatorial and
40 low-latitude F-layer was mainly perturbed by waves that were generated not far
41 away from the observed location or electric fields generated by the Equatorial
42 Electrojet (EEJ). On the contrary, during geomagnetic storms when the energy
43 sources are in high latitudes the waves (TIDs) travel a very long distance from high
44 latitude to equatorial region and electric fields can be mapped via magnetic field
45 lines. However, in the recent times an unexpected coupling between high latitude,
46 mid- latitude, and equatorial/low latitudes was discovered during sudden
47 stratospheric warming (SSW) events. All aspects involved in this process must be
48 explored in order to improve our knowledge about the Earth's atmosphere.

49

50 The day-to-day variability in the equatorial and low-latitude
51 ionosphere/thermosphere is one of highlighted topics of this investigation and
52 considerable research has gone into understanding the physics behind the
53 observed high variability, particularly in the F-layer ([Rishbeth et al., 2009](#);
54 [Fagundes et al., 2009](#)). It is well known that equatorial and low-latitude
55 ionosphere/thermosphere system is predominantly disturbed by waves (gravity
56 waves/ Medium-Scale Traveling Ionospheric Disturbances (MSTIDs), tides and
57 planetary waves) that are generated in the lower atmosphere or in-situ ([Fagundes](#)
58 [et al., 2005, 2009](#); [MacDougall et al., 2009](#); [Klausner et al., 2009](#)), solar radiation
59 (UV, EUV and X-ray) and sometimes by disturbed electric fields and TIDs
60 (Travelling Ionospheric Disturbances) generated during geomagnetic storms
61 ([Sahai et al., 2009](#); [de Abreu et al., 2010](#); [de Jesus et al., 2013](#)).

62

63 For several years, it was thought that, during geomagnetically quiet
64 conditions the equatorial and low-latitude F-layer was primarily perturbed either by
65 waves that were generated not far away from the observed location or by electric
66 fields generated from the Equatorial Electrojet (EEJ), via tidal winds, which are
67 transmitted along the magnetic field lines to equatorial F-region altitudes
68 ([Fagundes et al. 2009](#)). In contrast, during geomagnetic storms when energy
69 sources are in the high latitudes, the waves (TIDs) travel a very long distance from
70 the high latitude to the equatorial region and disturbed electric fields can be
71 mapped via magnetic field lines and, in turn, disturb the equatorial and low-latitude
72 F-layer ([de Abreu et al., 2010](#)).

73

74 Recently an unforeseen coupling between high latitudes, mid latitudes, and
75 equatorial/low latitudes at upper atmospheric/ionospheric altitudes was discovered
76 during sudden stratospheric warming (SSW) events ([Chau et al., 2010](#),
77 [Goncharenko et al., 2010a, 2010b](#)). Interestingly, [Resmi et al., \(2013\)](#) have
78 reported a coupling between polar and tropical stratosphere during SSW. They
79 have further reported the presence of a strong cooling in the entire tropics (30°N–
80 30°S) associated with SSW events and the cooling became intense of the order of
81 10–15°C during the peak phase of the SSW. The exploration of all aspects
82 involved in this process must be investigated in order to improve our knowledge of
83 the Earth’s upper atmosphere and ionosphere.

84

85 The present paper investigates the effects of the lower-upper atmosphere
86 vertical coupling at high latitude (Northern Hemisphere) on the equatorial, low- and
87 mid-latitude ionosphere (Southern Hemisphere), during a major SSW, which took
88 place in January-February 2009. Although the effect of the SSW on the
89 ionosphere/upper atmosphere has been studied by several researchers ([Chau et](#)
90 [al., 2010, 2012](#), [Goncharenko et al., 2010a, 2010b, 2013a, 2013b](#); [Liu et al., 2011](#);
91 [Pancheva and Mukhtarov 2011](#); [Bessarab et al., 2012](#); [Korenkov et al., 2012](#)), in
92 this investigation, the effects of the 2009 SSW in the South American sector have
93 been explored in more detail.

94

95 Using the large database from 17 GPS receivers and 2 ionosonde stations
96 spanning from 2.8°N to 53.81°S and 36.7°W to 67.8°W over the South American

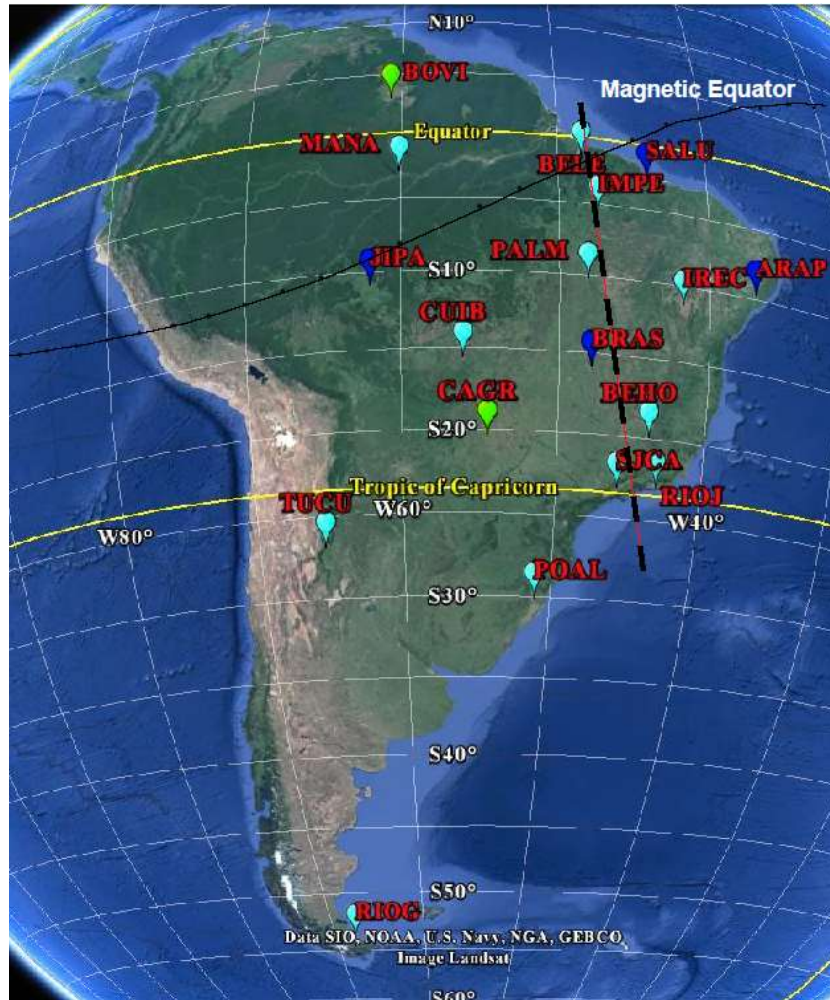
97 sector, the disturbances in the vertical Total Electron Content (VTEC) caused from
98 equator to the mid-latitudes during the SSW event have been studied and the
99 results are presented. Further, the variations in the Equatorial Ionization Anomaly
100 (EIA) have been studied.

101

102 **2. Observations**

103

104 In the present study, the stratospheric temperatures at 10hPa (~30km)
105 between 60° and 90° on the northern hemisphere have been obtained from the
106 NASA online data service [http://acdb-](http://acdb-ext.gsfc.nasa.gov/Data_services/met/ann_data.html)
107 [ext.gsfc.nasa.gov/Data_services/met/ann_data.html](http://acdb-ext.gsfc.nasa.gov/Data_services/met/ann_data.html). The dual frequency GPS
108 measurements from 17 receivers distributed from 2.8°N to 53.8°S latitudes and
109 from 36.7°W to 67.8°W longitudes over the South American sector during the
110 period from January to February 2009 have been used. These receivers are from
111 the network of the Instituto Brasileiro de Geografia e Estatística (IBGE) network of
112 GPS receivers ([http://www.ibge.gov.br/home/geociencias/geodesia/rbmc/](http://www.ibge.gov.br/home/geociencias/geodesia/rbmc/rbmc_est.php)
113 [rbmc_est.php](http://www.ibge.gov.br/home/geociencias/geodesia/rbmc/rbmc_est.php)). The TEC values are derived using the differential delay technique
114 using the dual frequency measurements at L1 and L2 frequencies over the
115 considered locations. Simultaneous ionosonde measurements over the Equatorial
116 Ionization Anomaly (EIA) crest locations, Tucuman (TUCU) and Sao Jose dos
117 Campos (SJCA) have also been used to study the variations of the F-layer peak
118 parameters during the considered SSW event. Figure 1 and Table 1 show the
119 geographical and geomagnetic locations of all these GPS and ionosonde receivers
120 over the South American sector.



122

123 Figure 1. South American map showing the locations of GPS and Digital
124 Ionosonde stations. The blue and green icons indicate stations that are
125 analyzed in more details. The GPS stations along the black colored
126 dashed line are used to study the EIA characteristics during the present
127 SSW event.

128

129

130

131 **Table 1-** Details of the GPS and digital ionosonde stations symbols, latitudes and
 132 longitudes sites used in the present investigation.

Site	Lat. Geog.	Lon. Geog.	Lat. Mag.	Lon. Mag
	+N	W	+N	E
GPS stations				
Boa Vista - BOVI	2.8	60.7	12.6	11.7
Belem - BELE	-1.4	48.5	7.8	23.9
São Luis - SALU	-2.6	44.2	6.3	28.1
Manaus - MANA	-3.0	60.1	12.8	12.3
Imperatriz - INPE	-5.5	47.5	3.7	24.6
Arapiaca - ARAP	-9.7	36.7	-1.4	34.9
Palmas - PALM	-10.2	48.2	-1.4	23.5
Ji-Paraná - JIPA	-10.9	62.0	-0.9	10.0
Irece - IREC	-11.2	41.9	-2.4	29.6
Cuiabá - CUIB	-15.6	56.1	-5.8	15.5
Brasília - BRAS	-15.9	47.9	-6.6	23.4
Belo Horizonte - BEHO	-19.9	43.9	-10.9	27.0
Campo Grande - CACR	-20.4	54.5	-10.7	16.8
Rio de Janeiro - RIOJ	-22.9	43.2	-13.9	27.4
S. J. Campos - SJCA	-23.2	45.9	-14.0	24.8
Porto Alegre - POAL	-30.1	51.1	-20.5	19.4
Rio Grande - RIOG	-53.8	67.8	-43.6	3.6
Ionosonde stations				

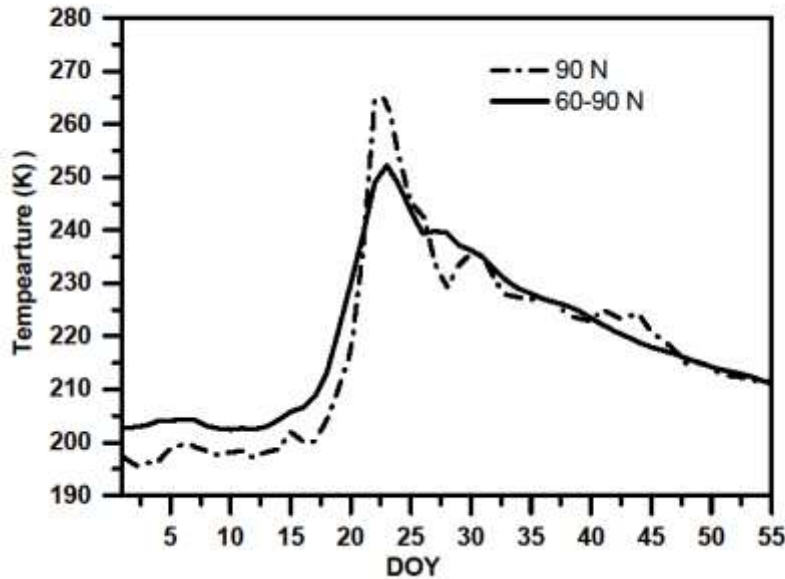
S. J. Campos - SJCA	-23.2	45.9	-14.6	24.7
Tucumán - TUCU	-26.9	65.4	-16.8	6.2

133

134 **3. Results and Discussion**

135

136 Figure 2 presents the average stratospheric temperatures from day 1 to 55
137 in the northern hemisphere. It is seen from this figure that the stratospheric
138 temperature at high latitude rapidly increases from January 11, 2009 (~200 K) to
139 January 23, 2009 (~250 K). After reaching a peak on 23rd January, 2009, the
140 temperature gradually decreases towards the end of February 28, 2009 and the
141 temperature reaches the typical quiet day value of nearly ~210 K. During this SSW
142 event, the solar activity was very low ($F_{10.7} \sim 68 \text{ W/m}^2 \text{ Hz}$) and geomagnetic
143 conditions are very quiet and the minimum Dst on January and February is around
144 -29 nT and -38 nT respectively. Hence, any ionospheric disturbance, in the
145 equatorial and low- and mid-latitude regions, during these 2 months are not related
146 to geomagnetic activity and could be due the effect of the SSW. The following
147 sections describe the response of the equatorial, low and mid latitude ionosphere
148 during the considered SSW event.



149

150 Figure 2. Plots showing the stratospheric temperatures at 90°N and 60°-90°N
 151 (averaged) at 10 hPa (~30 km) in the northern hemisphere during the
 152 period January-February, 2009.

153

154 3.1 VTEC at Equatorial and Low-Latitudes

155

156 Figure 3A presents the VTEC variations as a function of time (UT) and day
 157 of year (DOY) from January to February, 2009 at Sao Jose dos Campos (23°S, an
 158 EIA crest location). The white solid line shows the average stratospheric
 159 temperature variation between 60°N to 90°N at 10hPa (~30km) and vertical dashed
 160 lines indicate the disturbed days (DOY 23-27) due to the SSW. In order to avoid
 161 high frequency changes and ripples in VTEC, the two hours running average
 162 values have been calculated and presented.

163

164 The diurnal variations of VTEC over the low latitude stations during DOY 23,
165 24 are presented in Figure 3B and during DOY 25, 26 and 27 are presented in
166 Figure 3C. The mean diurnal variations of VTEC during 10 quiet days in the
167 considered period are plotted as gray bands in Figure 3B and C and the width of
168 this gray band represents the ± 1 standard deviation in VTEC values. It could be
169 mentioned here that the quiet day period was not affected by the SSW. It is seen
170 from this Figure that, during nighttime from 00:00 UT to 10:00 UT (21:00 to 07:00
171 LT) the VTEC varies around 2-15 TECu. After 10:00 UT (07:00 LT) the VTEC start
172 increasing due to solar radiation and fountain effect and reach a peak value of ~45
173 TECu around 17:00 UT (14:00 LT) and then start decreasing while a secondary
174 peak is observed around 20:00 - 21:00 UT (17:00 - 18:00 LT). This second VTEC
175 peak is due to the electric field pre-reversal enhancement that takes place just after
176 the sunset and its reinforce the EIA. It is important mention that the effects of the
177 electric field pre-reversal enhancement in the TEC, at low latitude, depend on
178 season and solar cycle (for more details see [Fagundes et al., 2009](#) and [Fejer et al.,
179 1979](#)).

180

181 A comparison between the diurnal variations of VTEC over low latitudes with
182 those of the quiet day averaged TEC (gray band), revealed that the VTEC values
183 show significant disturbances and the onset of the disturbance is coincident with
184 the SSW peak (Figure 3). It is seen from the contours presented in Figure 3A that
185 there is a significant decrease of the maximum daytime values of TEC during the
186 SSW event. The day maximum is observed around 16:00 UT during the SSW while
187 the peak is observed between 18:00 and 20:00 UT in the remaining days. A similar

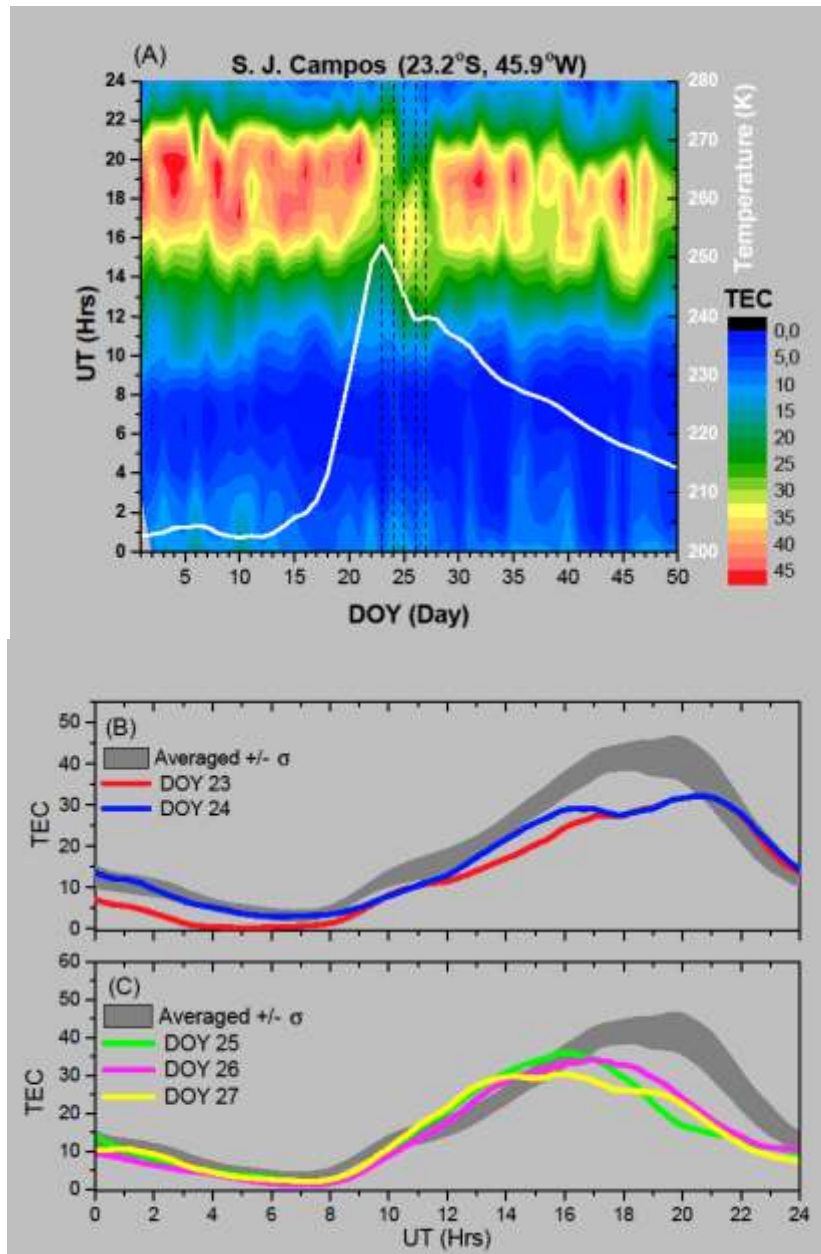
188 result has been reported by [Goncharenko et al. \(2010a\)](#) and [\(2010b\)](#); they noticed
189 that the low-latitude ionosphere perturbation persisted for several days after the
190 SSW peak.

191

192 It is observed from Figure 3B that the diurnal variations of VTEC during
193 DOY 23 and 24 are quite similar to those of the diurnal averaged quiet-day
194 variations (gray band). However, the daytime maximum values of VTEC during
195 DOY 23 and 24 are lower than the quiet-day averaged values from 08:00 UT to
196 21:00 UT (05:00 to 18:00 LT). The diurnal variation of TEC during quiet days show
197 the daytime TEC maximum around 45-50 TECu while the daytime maximum during
198 the SSW event is around 30-35 TECu indicating a significant decrease of about
199 35%.

200

201 The TEC values during the following three days from DOY 25 to 27 are
202 compared with the quiet day diurnal average TEC variations (gray band) in Figure
203 3C. During these 3 days the diurnal variations of TEC are not similar to the
204 averaged quiet-day variations. The main difference is in the occurrence of the day
205 maximum TEC. It is observed that the averaged quiet-day reaches its maximum
206 around 18:00 to 20:00 UT (15:00 to 17:00 LT) during the quiet days while the
207 diurnal variation of TEC during the SSW, shows its maximum around 15:00 to
208 17:00 UT (12:00 to 14:00 LT). Nevertheless, from 16:00 UT to 24:00 UT (13:00 to
209 21:00 LT) the VTEC values during these three days (DOY 25-27) are lower than
210 those of the quiet-day (about 10 TEC units).



211

212

213 Figure 3. (A) Contour plot showing the VTEC variations with UT as a function of
 214 DOY (January-February, 2009) at Sao Jose dos Campos (23oS, near the
 215 EIA crest). The white solid line shows the average stratospheric
 216 temperature variations between 60°N to 90°N at 10hPa (~30km), and the
 217 dashed lines indicate the DOY from 23 to 27. (B). The VTEC diurnal
 218 variations during disturbed days (DOY 23 and 24). The averaged quiet-

219 day VTEC is shown as gray bands with the band widths indicating ± 1
220 standard deviation. (C) The same as (B) but for DOY 25, 26, and 27.

221

222 During 2009 the solar activity was very low and the VTEC from 24 UT to
223 11:00 UT in the morning was very low (VTEC < 15); considerable variations in
224 VTEC are not observed during this time. However, after 12 UT when the VTEC
225 increases significant changes are observed due to the effect of the SSW. Hence, in
226 order to highlight the VTEC changes during the 2009 SSW event, the VTEC
227 variations with UT as a function of DOY from 09:00 UT to 24:00 UT at 16 different
228 locations are presented in Figures 4A and 4B.

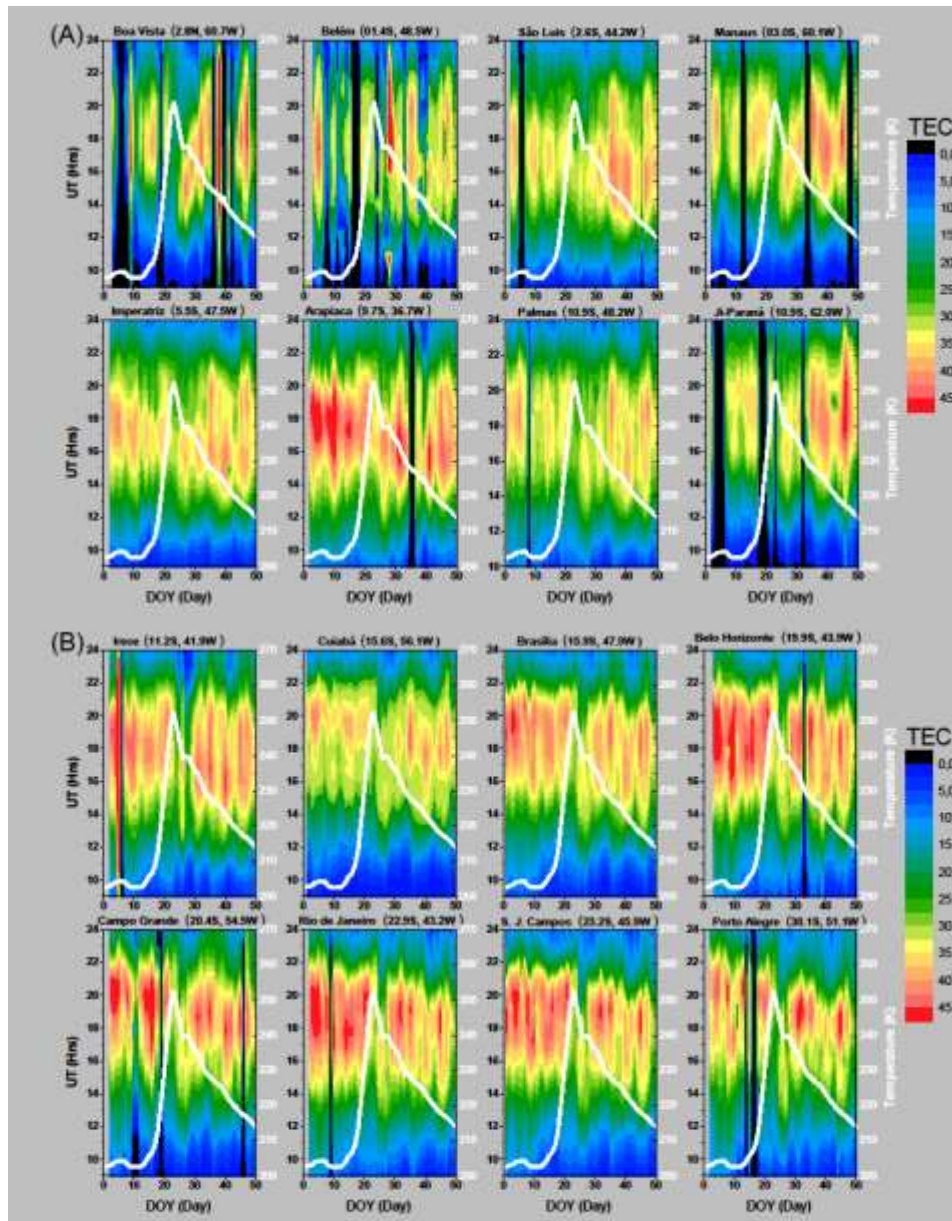
229

230 The contours presented in Figure 4 clearly indicate the SSW disturbance
231 effect in VTEC beginning in all 16 stations on DOY 23, just when the SSW reached
232 its maximum temperature and continuing for the next five-six days. Each station
233 has its particular response to the SSW disturbances, with different strength and
234 time of duration. However, it is very clear that the VTEC was perturbed during 5 or
235 6 days in all 16 stations indicating that the SSW event in the northern hemisphere
236 significantly influenced the electron density variations over the equatorial and low
237 latitudes in the southern hemisphere.

238

239 Significant portion of differences between different stations is most likely
240 related to the location of the station with regards to the location of the equatorial
241 ionization anomaly. Earlier studies have demonstrated that largest variations in
242 VTEC during SSW are observed at the crests of the EIA (Goncharenko et al.,

243 2010a, Liu et al., 2011), and location of the crests can vary periodically by several
244 degrees in latitude (Mo et al., 2014). In addition, the difference from one station to
245 another is probably related with a local perturbation caused by MSTIDs and/or
246 PWs disturbances. Since the geographical extent covered by the 16 stations is
247 very large, 32.9o in latitude and 25.3o in longitude, it can be expected that the
248 VTEC in each station is subject to different MSTIDs local sources disturbance or
249 closed stations are subject to similar PW disturbances, but with different phases.
250 The disturbance effects (SSW, MSTIDs, and PWs) are probably superimposed, but
251 the effect of the SSW is very strong and global because the main feature of the
252 disturbance is present in all 16 stations.



253

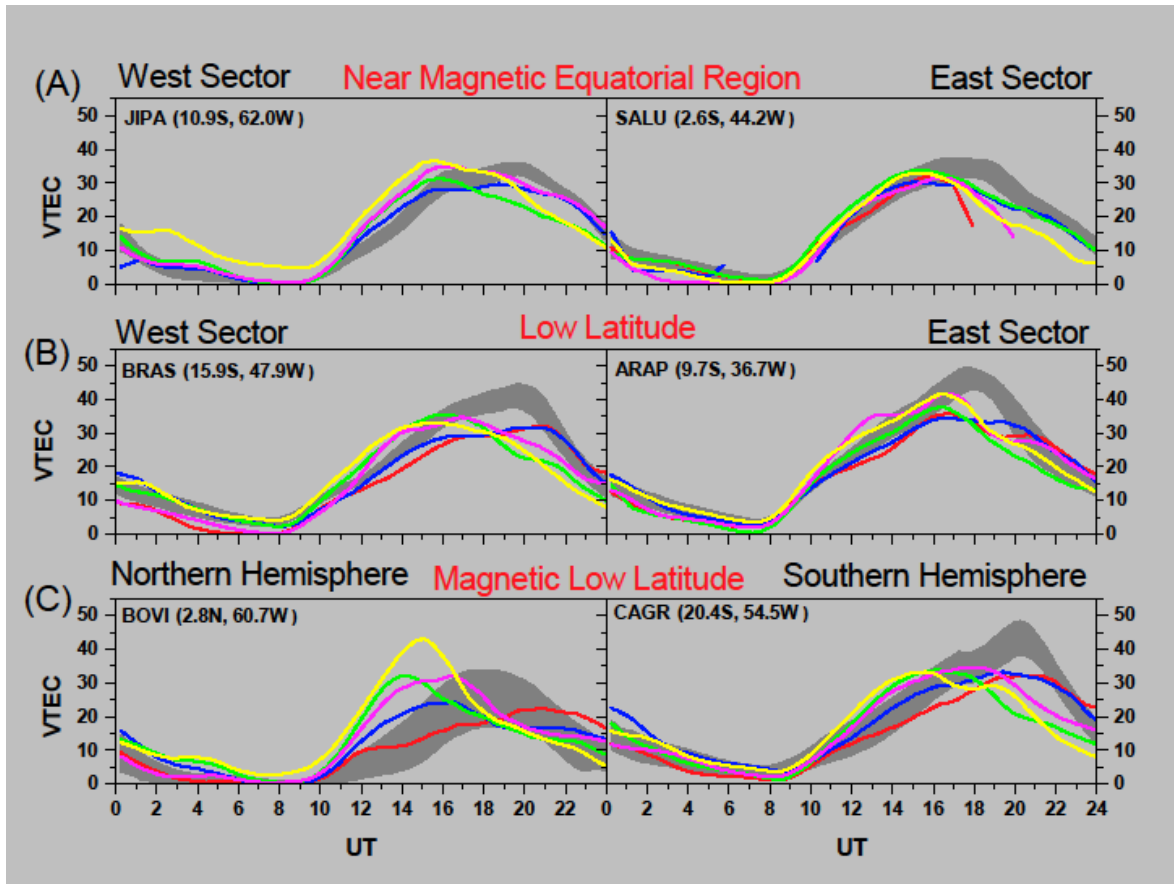
254

255 Figure 4. (A) VTEC variations with UT as a function of day of the year (January-
 256 February, 2009) for 8 stations over Brazilian sector, spanning from
 257 latitude 2.8°N to 10.9°S and longitude from 36.7°W to 62.0°W. (B) VTEC
 258 variation with UT as a function of day of the year (January-February,
 259 2009) for 8 stations over Brazilian sector, spanning from latitude 11.2°S to
 260 30.1°S and longitude 41.9°W to 56.1°W. The white solid lines show the

261 stratospheric temperature averaged between 60°N to 90°N at 10hPa
262 (~30km).

263

264



265

266 Figure 5. (A) The averaged quiet-day diurnal VTEC variations is shown as gray
267 bands with the band widths indicating ± 1 standard deviation and the
268 variation of VTEC during the disturbed period (DOY 23 to 27) over near
269 magnetic equatorial region (Ji-Parana - JIPA and Sao Luis - SALU). (B)
270 The same as (A) but for low-latitude (Brasilia - BRAS and Arapiaca -
271 ARAP). (C) The same as (A) but for Boa Vista (BOVI) located in the

272 magnetic North Hemisphere and Campo Grande (CAGR) located in the
273 South Hemisphere.

274

275 Figure 5A and 5B show the mean diurnal variations of TEC over two near
276 magnetic equatorial stations and two low latitude stations during the SSW event of
277 DOY 23 to 27. The simultaneous quiet day mean values of TEC along with the ± 1
278 standard deviations have been plotted as grey bands for comparison. It is
279 important to mention here that the two near equatorial stations (JIPA and SALU)
280 are separated by 18° in longitude and the two low latitude stations (BRAS and
281 ARAP) are separated by 11° in longitude. These stations are represented with blue
282 colored icon in Figure 1. In general, the quiet day VTEC variations over the
283 equatorial and low latitudes show higher values in the afternoon hours. The diurnal
284 variations of quiet day averaged TEC show the daytime maximum of about 50
285 TECu over the low latitudes while it is less (around 35 TECu) over the equatorial
286 regions. This is due to the well-known phenomena of the fountain effect under
287 which the uplift of the equatorial F-layer takes place and the plasma over the
288 equator is carried to low latitudes causing an increase in the low latitude electron
289 density.

290

291 The diurnal variations of TEC during DOY 23 to 27 show that the equatorial
292 regions are less affected by SSW compared to that of the low latitudes. However, a
293 decrease in the TEC values is observed at both equatorial stations after 16:00 UT
294 when compared with the quiet day average TEC variations. Prominent influence of
295 SSW is observed over the low latitude stations. The daytime maximum TEC

296 observed during the disturbed days is broad varying between 35 to 40 TECu and it
297 is much less compared to those of the quiet day which varies between 45 to 50
298 TECu around 17:00 UT.

299

300 Figure 5C shows the diurnal variations of VTEC at two magnetic low-latitude
301 stations (BOVI and CACR) one in northern and another one in the southern
302 hemisphere, which are separated by about 23° latitude. These stations are shown
303 in Figure 1 with green icon. From the observations over these two stations it can be
304 observed that the VTEC in northern hemisphere was more affected by the SSW
305 than the VTEC in southern hemisphere. These hemispheric differences can be
306 attributed to the reason that the SSW occurred in the high latitude northern
307 hemisphere. The strong latitudinal dependence and hemispheric asymmetry of the
308 TEC disturbances observed in the present study during SSW are in agreement
309 with those reported earlier by [Liu et al. \(2011\)](#). However, the present study reveals
310 the important characteristics such as, latitudinal and hemispheric differences due
311 to SSW events with quantitative database in the South American sector.

312

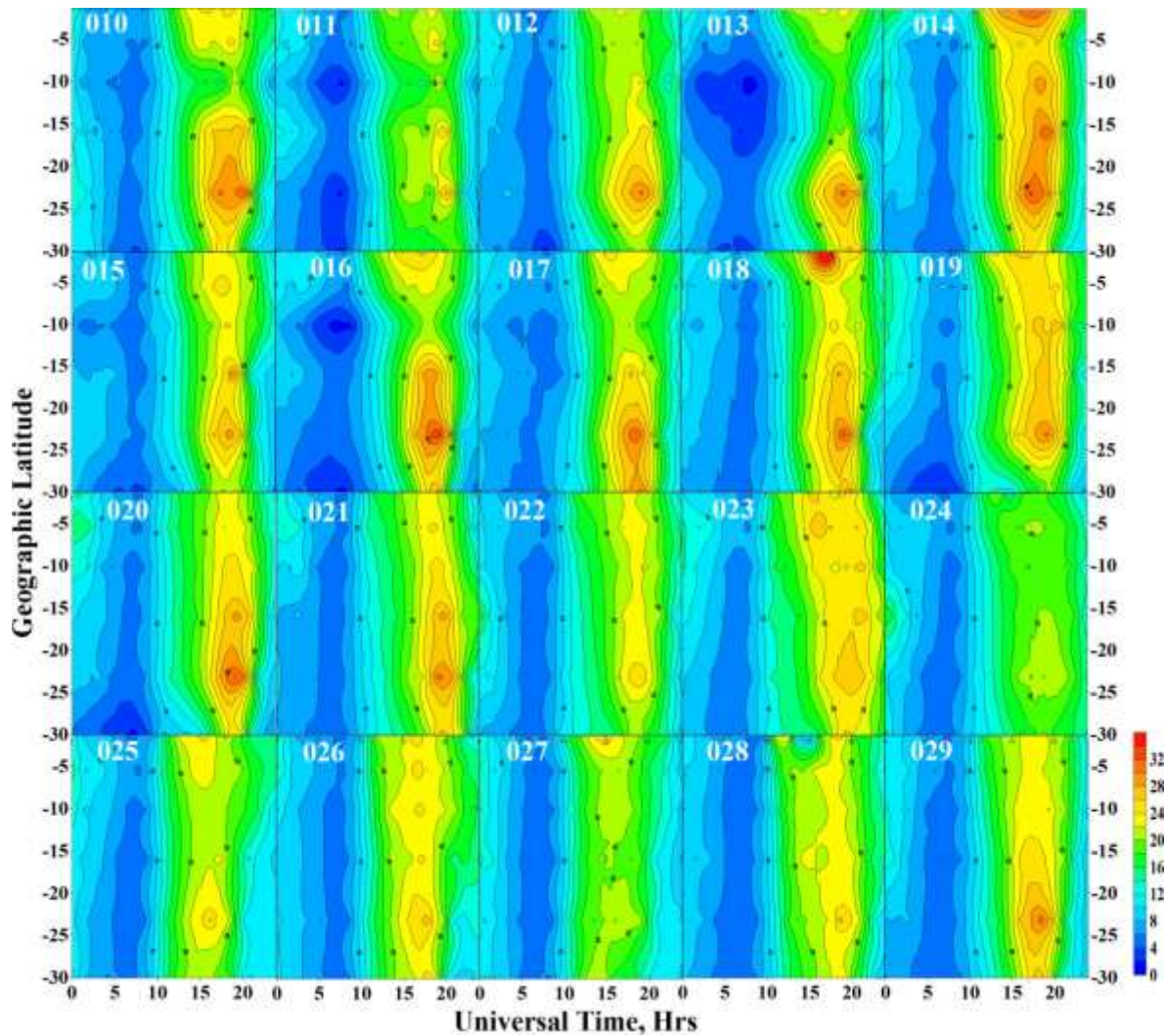
313 A perusal of Figures 3A and 3B indicates that the electron density at the
314 anomaly crest locations in the South America sector was perturbed by the SSW
315 event. In addition, recently [Goncharenko et al. \(2010a\)](#) reported that, after the peak
316 in stratospheric temperature an enhancement of the EIA in the morning sector and
317 a suppression of the EIA in the afternoon sector are observed. Hence, in order to
318 investigate the day-to-day variability in the formation of EIA before and during the
319 SSW event the TEC data from a set of seven GPS receivers from equator to the

320 anomaly crest location and beyond are considered. The stations used in this
321 investigation are shown along the black coloured dashed line in Figure 1. Contour
322 plots showing the day-to-day variations of the EIA over the South American sector
323 from DOY 10 to 29 are presented in Figure 6. In general, it is seen from this Figure
324 that the EIA shows significant variability from one day to the other.

325

326 The high variability of the EIA is expected, but the formation of the EIA is
327 usually observed around 20° - 25° S. However, from DOY 22 to DOY 28 the EIA
328 was perturbed, with perturbations seen as suppression of EIA lasting several days
329 and shift of the daytime peak to earlier hours (in particular, on days 25-26).
330 According to [Fejer et al. \(1979\)](#) the equatorial electric fields, which control the F-
331 layer vertical drift are the result of a complicated interaction between the E-and F-
332 region. The E region dynamo fields are created by tidal winds in the E-layer and
333 are coupled to the F-region via the nearly equipotential magnetic field lines. Since
334 the EIA were suppressed during several days during the SSW, the changes in the
335 EIA and the suppression of the anomaly observed in the present study during the
336 SSW event can be produced by the changes in the E-region electric fields and tidal
337 winds at E-region altitudes.

338



339

340 Figure 6. Contour plots showing the daily VTEC variation as a function of
 341 geographic latitude and UT from DOY 10 to DOY 29. The latitude starts
 342 from equator to the EIA crest in the southern hemisphere and beyond.

343

344 3.2 Ionosonde measured $h'F$ and foF2 variations at Low-Latitude

345

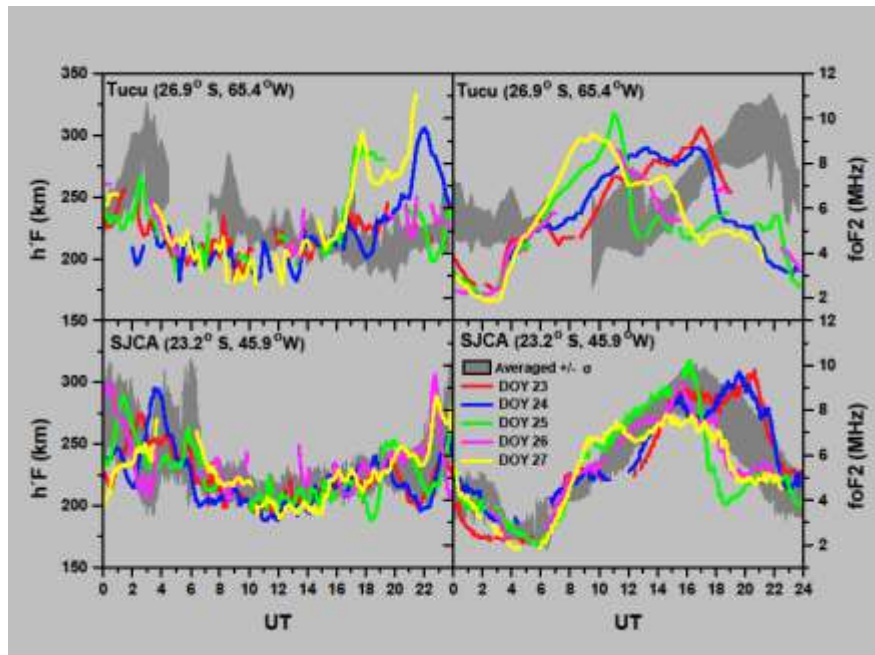
346 Figure 7 shows the variations of $h'F$ and foF2 during the SSW period (DOY
 347 23 to 27) observed at TUCU and SJCA. The diurnal variations of quiet day
 348 averaged values of $h'F$ (ionospheric F region base height) and foF2 are shown as

349 gray bands. A perusal of Figure 7 (left panels) indicates that, in general, the
350 variations of h'F during the DOY 23 to 27 closely follow the quiet-day averaged
351 variations at both stations TUCU and SJCA, except over TUCU during some short
352 intervals (DOY 24, 25 and 27), where an increase in the h'F up to 50-75km is seen
353 compared to that of the quiet day median values from ~18:00 to 24:00 UT. This
354 increase is followed by a smaller decrease in h'F at 2-4 UT. [Sumod et al. \(2012\)](#)
355 reported an alternating increase and decrease of h'F in the evening hours over the
356 Indian sector during the SSW of January 2008 period. In addition, they pointed out
357 that the strengthening of the Pre-Reversal Enhancement (PRE) may be associated
358 with the SSW. In the present work, a similar behavior is noticed during DOY 24, 25
359 and 27 only in the American west-sector (TUCU).

360

361 The foF2 presented in the right panels of Figure 7 during DOY 23 to 27 do
362 not follow the quiet-day averaged variations. The foF2 deviations from median
363 values are stronger at TUCU than SJCA. This indicates strong east-west
364 differences in the ionospheric response to the SSW event. Nevertheless, in both
365 the stations, the SSW lead a decrease and increase of foF2 compared with
366 averaged quiet-day variations. The decrease in foF2 occurs in the afternoon and
367 evening/nighttime sector (16:00 UT – 04:00 UT) and reaches 2-6 MHz, while
368 increase of varying magnitude is observed mostly in the morning sector. The
369 observations in the South American sector are quite different than those observed
370 in the Indian sector ([Sumod et al., 2012](#)). The present study carried out over the
371 South American sector reveals strong foF2 disturbances compared with those of
372 the quiet day variations while these disturbances are weaker (~1 MHz) and not as

373 long-lasting in the Indian sector. It is not clear if stronger disturbances in the
374 American longitudinal sector are related to the strength of the SSW event, which is
375 more intense in January 2009 as compared to January 2008. However, earlier
376 studies of the same events have reported that ionospheric perturbations caused by
377 SSW are stronger in the American sector than in the Asian sector for January 2009
378 SSW event (Goncharenko et al., 2010b, Liu et al., 2011), and stronger than in the
379 Asian and African sector for January 2013 SSW event (Goncharenko et al., 2013).
380 Our observations provide additional evidence of significant longitudinal variations in
381 ionospheric response to SSW.
382



383
384 Figure 7. Variations of h'F and FoF2 during the period from DOY 23 to DOY 27 at
385 Tucuman (TUCU) and Sao Jose dos Campos (SJCA). The averaged
386 quiet-day h'F and foF2 values are shown as gray bands with the band
387 widths indicating ± 1 standard deviation.

388

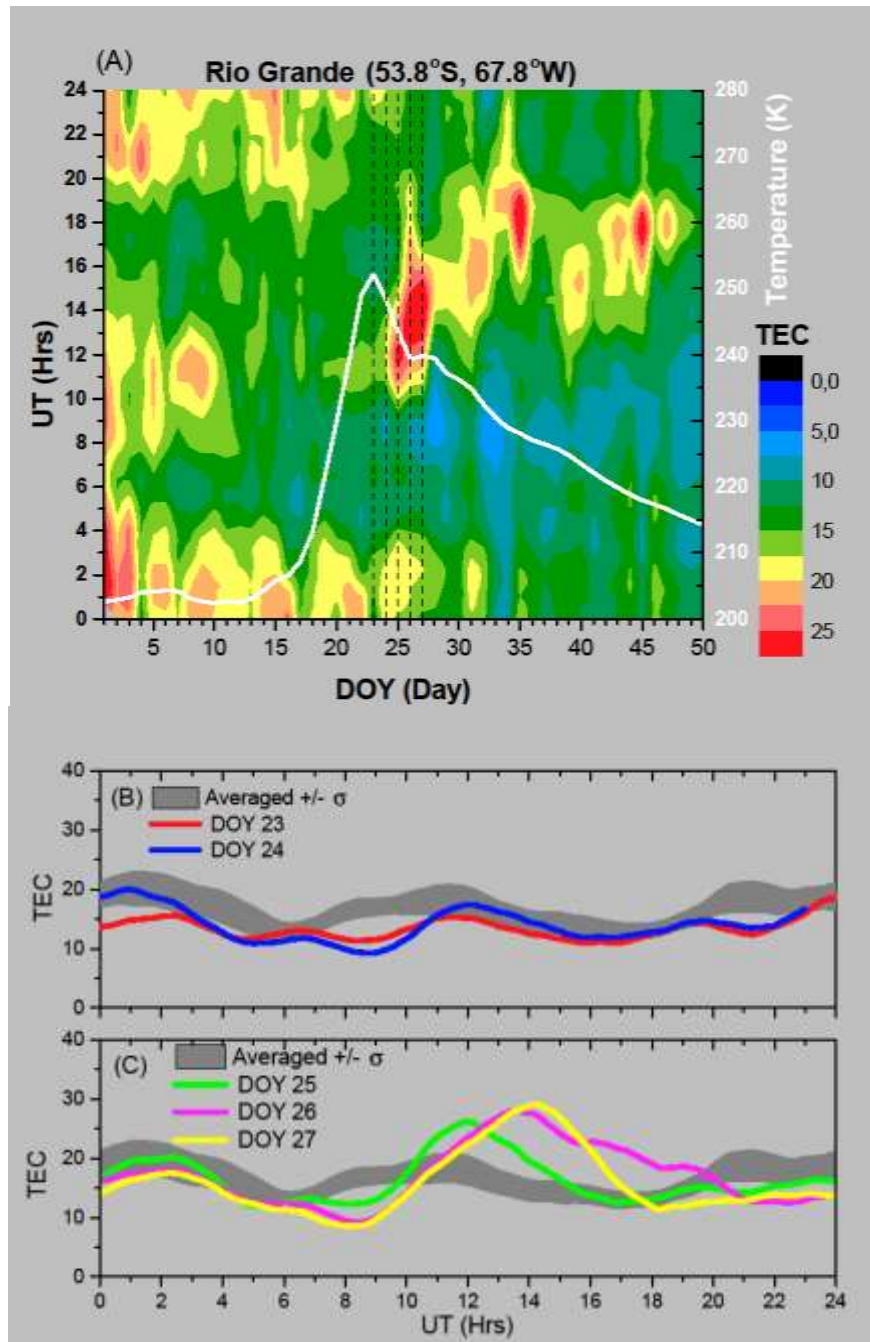
389 **3.3 VTEC at Mid-Latitude**

390 From the above results, it can be observed that the equatorial and low-
391 latitude ionosphere in the southern hemisphere is significantly disturbed by the
392 2009 SSW event in the northern hemisphere. Since the disturbances reach up to
393 the equatorial and low-latitudes, some ionospheric coupling between low- and mid-
394 latitudes should be expected. Therefore, the VTEC variations over Rio Grande
395 (53.8°S) have been studied to understand the mid-latitude ionospheric response
396 for the SSW event. The contour plot presented in Figure 8A shows the day-to-day
397 variations of VTEC as a function of DOY and UT, during January-February 2009
398 (summer season) in the southern hemisphere. It is readily observed from this
399 Figure that the VTEC is strongly disturbed during day-time (10:00 to 16:00 UT) for
400 several days (DOY 24 to DOY 28). During this time, VTEC over Rio Grande
401 increases almost by a factor of 2 (from 10-15 TECu to ~25TECu). In addition, the
402 disturbance lasts for several days after DOY 28 (DOY 29-36), although it becomes
403 weaker and shifts to later local times.

404

405 The quiet day averaged diurnal variations of TEC are presented in Figure 8 B and
406 C as gray bands and the thickness of these bands represent the \pm standard
407 deviation of VTEC. We note that quiet-time VTEC at this time does not present
408 strong day-to-night variations. The colored lines are the diurnal variation of the
409 TEC during disturbed days (DOY 23 and 24 are in Figure 8B and DOY 25-27 are in
410 Figure 8C). Comparing the VTEC variations during disturbed days with those of the
411 averaged quiet-day diurnal variation reveals that, on the DOY 23 and 24, the

412 disturbances are moderate. The VTEC variations during DOY 25 to 27 show large
413 deviations compared to the quiet day averaged variations, with daytime (13-16 UT)
414 increase up to a factor of 2 (10-15 TECu), and nighttime-to-morning (7-9UT)
415 decrease by 5-7 TECu. These strong variations observed in the VTEC over Rio
416 Grande are surprising since the SSW is in the northern hemisphere. For the strong
417 variations to occur in the Southern Hemisphere, the SSW's influence must have
418 propagated up to the mid-latitudes in the opposite (southern) hemisphere. This
419 highlights the importance of studying the changes in the ionosphere due to SSW in
420 a broad range of latitudes, since a single stratospheric event at high latitudes in the
421 Northern Hemisphere is disturbing the whole ionosphere, suggesting that the SSW
422 produces ionospheric perturbations from Pole to Pole.



423

424

425 Figure 8. (A) VTEC variations with UT as a function of DOY (January-February,
 426 2009) at Rio Grande (53.8°S, mid-latitude), the white solid line show the
 427 average stratospheric temperature variation between 60°N to 90°N at
 428 10hPa (~30km), and the dashed lines indicate the DOY from 23 to 27.
 429 (B) The averaged quiet-day VTEC is shown as gray bands with the band

430 widths indicating ± 1 standard deviation and the variation of VTEC during
431 the disturbed period of DOY 23 and 24. (C) The same as (B) but for
432 DOY 25, 26, and 27.

433

434 **4. Conclusions**

435 In the present investigation, VTEC measurements from dual frequency GPS
436 receivers over 17 GPS locations covering a large geographical area from 2.8°N to
437 53.8°S latitudes and 36.7°W to 67.8°W longitudes in the South American sector
438 have been used to study the ionospheric response to the January-February 2009
439 SSW event. The ionosonde measurements over two typical anomaly crest
440 locations have also been used. The main objective of the present study is to
441 simultaneously investigate the ionospheric response at equatorial, low and mid-
442 latitudes as well as the variability in the EIA characteristics. The results observed in
443 the present investigation are summarized below.

444

445 a) After the occurrence of the peak in the stratospheric temperature in the
446 present 2009 SSW event, a large disturbance has been observed at all of the 16
447 different locations from equator to the low latitudes in the Southern Hemisphere.
448 These disturbances are found to be retained for a long duration of about five to six
449 days.

450

451 b) In general, the strength of the EIA crest shows large day-to-day variability
452 and the EIA is found to be suppressed during the SSW event.

453

454 c) The ionosonde measured h'F and foF2 also show significant deviations from
455 the mean quiet day variations. These deviations are largest in the afternoon-
456 evening hours, reaching 50-70km for h'F and 5-6 MHz for foF2. These American-
457 longitude disturbances are found to be stronger than those reported by [Sumod et](#)
458 [al., \(2012\)](#) in the Indian sector.

459

460 d) The VTEC variations in the southern mid-latitudes (53.8°S, Magnetic 43.6°
461 S) have also shown significant disturbances during the present Northern SSW
462 event. This highlights the importance of the investigations on ionospheric response
463 to the stratospheric warming since the SSW event in one hemisphere can create
464 strong perturbations in the ionosphere from one pole to the other.

465

466 **Acknowledgments:** The authors thank the authorities of the “Rede Brasileira de
467 Monitoramento Contínuo de GPS (RBMC)” operated by the “Instituto Brasileiro de
468 Geografia e Estatística (IBGE)”, Brazil, for kindly allowing us to use the data
469 obtained by the RBMC. The authors also thank the Brazilian funding agencies
470 FAPESP grant N° 2012/08445-9 and CNPq grants N° 302927/2013-1 and N°
471 457129/2012-3 for the partial financial support.

472

473 **References**

474

475 Bessarab FS; Korenkov YN; Klimenko MV; Klimenko VV; Karpov IV; Ratovsky KG;
476 Chernigovskaya MA Modeling the effect of sudden stratospheric warming within

477 the thermosphere-ionosphere system. J. Atmos. Solar Terr. Phys., V 90-91, 77-
478 85, DOI: 10.1016/j.jastp.2012.09.005, 2012.

479

480 Chau, JL; Aponte, NA; Cabassa, E; Sulzer, MP; Goncharenko, LP; Gonzalez, SA
481 Quiet time ionospheric variability over Arecibo during sudden stratospheric
482 warming events. JOURNAL OF GEOPHYSICAL RESEARCH-SPACE
483 PHYSICS, 115, A00G06, DOI: 10.1029/2010JA015378, 2010.

484

485 Chau, JL; Goncharenko, LP; Fejer, BG; Liu, HL Equatorial and Low Latitude
486 Ionospheric Effects During Sudden Stratospheric Warming Events Ionospheric
487 Effects During SSW Events. SPACE SCIENCE REVIEWS, 168 (1-4), 385-417
488 DOI: 10.1007/s11214-011-9797-5, 2012.

489

490 de Abreu AJ; Fagundes PR; Sahai Y; de Jesus R; Bittencourt JA; Brunini C; Gende
491 M; Pillat VG; Lima WLC; Abalde JR; Pimenta AA Hemispheric asymmetries in
492 the ionospheric response observed in the American sector during an intense
493 geomagnetic storm. J. Geophys. Res., 115(A12312), DOI:
494 10.1029/2010JA015661, 2010.

495

496 de Jesus R; Sahai Y; Fagundes PR; de Abreu AJ; Brunini C; Gende M; Bittencourt,
497 JA; Abalde JR; Pillat, VG Response of equatorial, low- and mid-latitude F-region
498 in the American sector during the intense geomagnetic storm on 24-25 October
499 2011. Adv. Space Res., 52(1), 147-157, DOI: 10.1016/j.asr.2013.03.017, 2013.

500

501 Fagundes PR; Pillat VG; Bolzan MJA; Sahai Y; Becker-Guedes F; Abalde JR;
502 Aranha SL; Bittencourt JA Observations of F layer electron density profiles
503 modulated by planetary wave type oscillations in the equatorial ionospheric
504 anomaly region. J. Geophys. Res., A12(A12302), DOI: 10.1029/2009JA014390,
505 2005.

506

507 Fagundes PR; Bittencourt JA; Abalde JR; Sahai Y; Bolzan MJA; Pillat VG; Lima
508 WLC F layer postsunset height rise due to electric field prereversal
509 enhancement: 1. Traveling planetary wave ionospheric disturbance effects. J.
510 Geophys. Res., 114 (A12321), 10.1029/2009JA014390, 2009.

511

512 Fejer BG; Farley DT; Woodman RF; Calderon C Dependence of equatorial f-region
513 vertical drifts on season and solar-cycle. J. Geophys. Res, 84(A10), 5792-5796,
514 DOI: 10.1029/JA084iA10p05792, 1979.

515

516 Goncharenko LP; Coster AJ; Chau JL; Valladares CE Impact of sudden
517 stratospheric warmings on equatorial ionization anomaly. J. Geophys. Res., 115
518 (A00G07), DOI: 10.1029/2010JA015400, 2010a.

519

520 Goncharenko LP; Chau JL; Liu HL; Coster AJ Unexpected connections between
521 the stratosphere and ionosphere. Geophys. Res. Lett., Volume: 37 Article
522 Number: L10101 DOI: 10.1029/2010GL043125, 2010b.

523

524 Goncharenko L; Chau JL; Condor P; Coster A; Benkevitch L Ionospheric effects of
525 sudden stratospheric warming during moderate-to-high solar activity: Case study
526 of January 2013. *Geophys. Res. Lett.*, 40(19), 4982-4986, DOI:
527 10.1002/grl.50980, 2013a.

528

529 Goncharenko LP; Hsu VW; Brum CGM; Zhang SR; Fentzke JT Wave signatures
530 in the midlatitude ionosphere during a sudden stratospheric warming of January
531 2010. *J. Geophys. Res.*, 118(1), 472-487, DOI: 10.1029/2012JA018251, 2013b.

532

533 Klausner V; Fagundes PR; Sahai Y; Wrasse CM; Pillat VG; Becker-Guedes F
534 Observations of GW/TID oscillations in the F2 layer at low latitude during high
535 and low solar activity, geomagnetic quiet and disturbed periods. *J. Geophys.*
536 *Res*, 114 (A02313), DOI: 10.1029/2008JA013448, 2009.

537

538 Korenkov YN; Klimenko VV; Klimenko MV; Bessarab FS; Korenkova NA; Ratovsky
539 KG; Chernigovskaya MA; Shcherbakov AA; Sahai Y; Fagundes PR; de Jesus R;
540 de Abreu, AJ; Condor P The global thermospheric and ionospheric response to
541 the 2008 minor sudden stratospheric warming event. *J. Geophys. Res*, 117
542 (A10309), DOI: 10.1029/2012JA018018, 2012.

543

544 Liu HX; Yamamoto M; Ram ST; Tsugawa T; Otsuka Y; Stolle C; Doornbos E;
545 Yumoto K; Nagatsuma T Equatorial electrodynamic and neutral background in
546 the Asian sector during the 2009 stratospheric sudden warming. *J. Geophys.*
547 *Res.*, 116(A08308), DOI: 10.1029/2011JA016607, 2011.

548

549 MacDougall J; Abdu MA; Batista I; Fagundes PR; Sahai Y; Jayachandran PT On
550 the production of traveling ionospheric disturbances by atmospheric gravity
551 waves. *J. Geophys. Res.*, 71(17-18), 2013-2016, DOI:
552 10.1016/j.jastp.2009.09.006, 2009.

553

554 Mo, X. H., Zhang, D. H., Goncharenko, L. P., Hao, Y. Q., and Xiao, Z.: Quasi-16-
555 day periodic meridional movement of the equatorial ionization anomaly, *Ann.*
556 *Geophys.*, 32, 121-131, doi:10.5194/angeo-32-121-2014, 2014.

557 Pancheva, D; Mukhtarov, P Stratospheric warmings: The atmosphere ionosphere
558 coupling paradigm. *J. Atmos. Solar Terr. Phys.*, 73(13),1697-1702, DOI:
559 10.1016/j.jastp.2011.03.006, 2011.

560

561 Resmi EA; Mohanakumar K; Appu KS Effect of polar sudden stratospheric
562 warming on the tropical stratosphere and troposphere and its surface signatures
563 over the Indian region. *J. Atmos. Solar Terr. Phys.*, 105, 15-29, DOI:
564 10.1016/j.jastp.2013.07.003, 2013.

565

566 Rishbeth H, Mendillo M, Wroten J, Roble RG Day-by-day modelling of the
567 ionospheric F2-layer for year 2002. *J. Atmos. Solar Terr. Phys.*, 71(2009), 848–
568 856, 2009.

569

570 Sahai Y; Becker-Guedes F; Fagundes PR; de Abreu AJ; de Jesus R; Pillat VG;
571 Abalde JR; Martinis CR; Brunini C; Gende M; Huang CS; Pi X; Lima WLC;

572 Bittencourt JA; Otsuka Y Observations of the F-region ionospheric irregularities
573 in the South American sector during the October 2003 'Halloween Storms'. Ann.
574 Geophys., 27(12), 4463-4477, 2009.

575

576 Sumod, SG; Pant, TK; Jose, L; Hossain, MM; Kumar, KK Signatures of Sudden
577 Stratospheric Warming on the Equatorial Ionosphere-Thermosphere System.
578 PLANETARY AND SPACE SCIENCE, 63-64, 49-55, DOI:
579 10.1016/j.pss.2011.08.005, 2012.

580

581

582

583 **Table Captions**

584 **Table 1-** Details of the GPS and digital ionosonde symbols, latitudes and
 585 longitudes sites used in the present investigation.

586

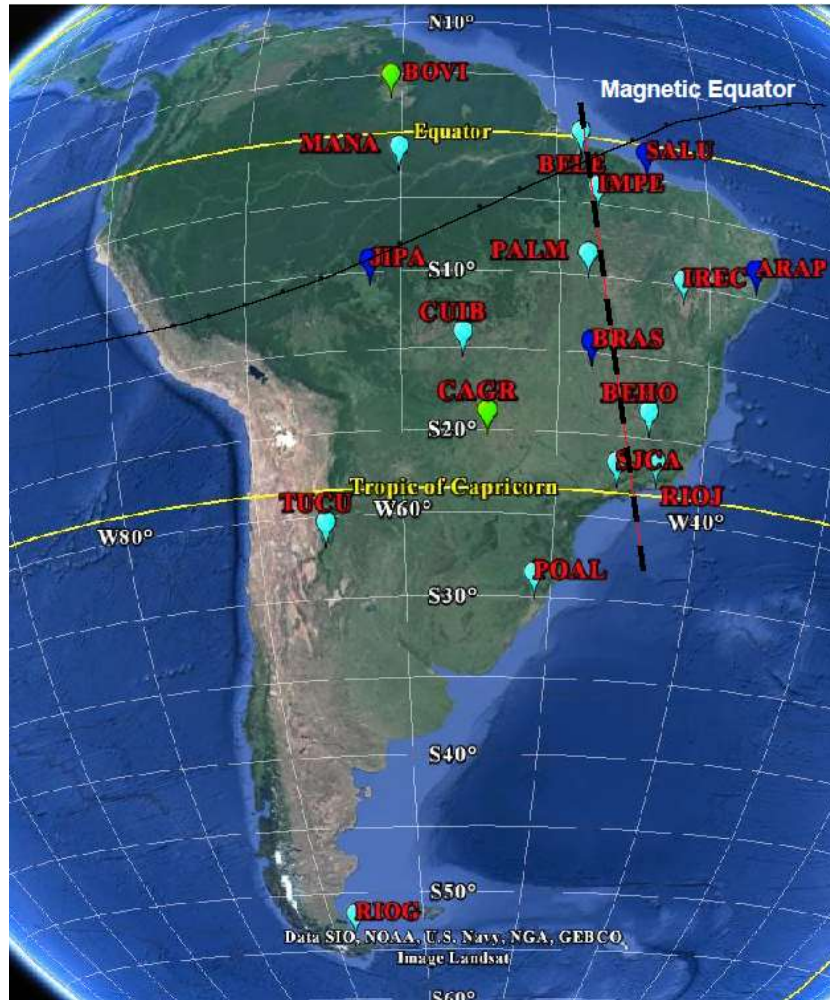
Site	Lat. Geog.	Lon. Geog.	Lat. Mag.	Lon. Mag
	+N	W	+N	E
GPS stations				
Boa Vista - BOVI	2.8	60.7	12.6	11.7
Belem - BELE	-1.4	48.5	7.8	23.9
São Luis - SALU	-2.6	44.2	6.3	28.1
Manaus - MANA	-3.0	60.1	12.8	12.3
Imperatriz - INPE	-5.5	47.5	3.7	24.6
Arapiacá - ARAP	-9.7	36.7	-1.4	34.9
Palmas - PALM	-10.2	48.2	-1.4	23.5
Ji-Paraná - JIPA	-10.9	62.0	-0.9	10.0
Irece - IREC	-11.2	41.9	-2.4	29.6
Cuiabá - CUIB	-15.6	56.1	-5.8	15.5
Brasília - BRAS	-15.9	47.9	-6.6	23.4
Belo Horizonte - BEHO	-19.9	43.9	-10.9	27.0
Campo Grande - CACR	-20.4	54.5	-10.7	16.8
Rio de Janeiro - RIOJ	-22.9	43.2	-13.9	27.4
S. J. Campos - SJCA	-23.2	45.9	-14.0	24.8
Porto Alegre - POAL	-30.1	51.1	-20.5	19.4

Rio Grande - RIOG	-53.8	67.8	-43.6	3.6
Ionosonde stations				
S. J. Campos - SJCA	-23.2	45.9	-14.6	24.7
Tucumán - TUCU	-26.9	65.4	-16.8	6.2

587

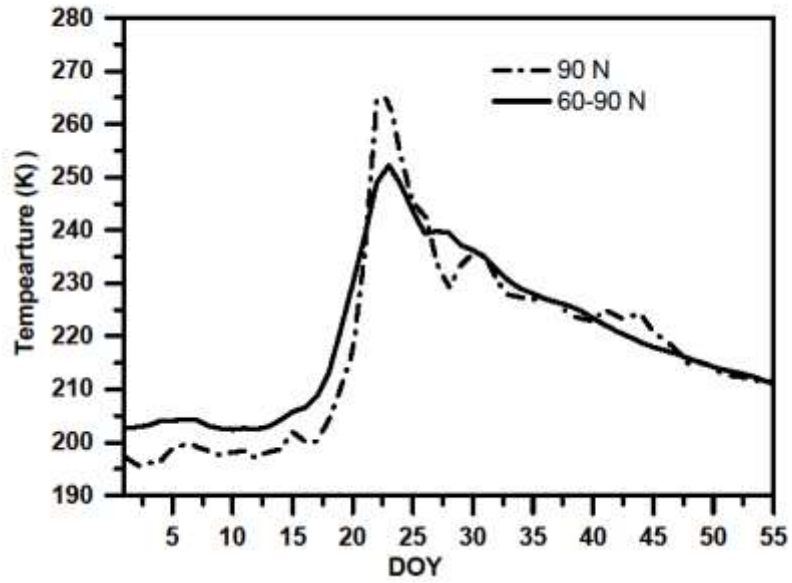
588

589 **Figures Captions**



590

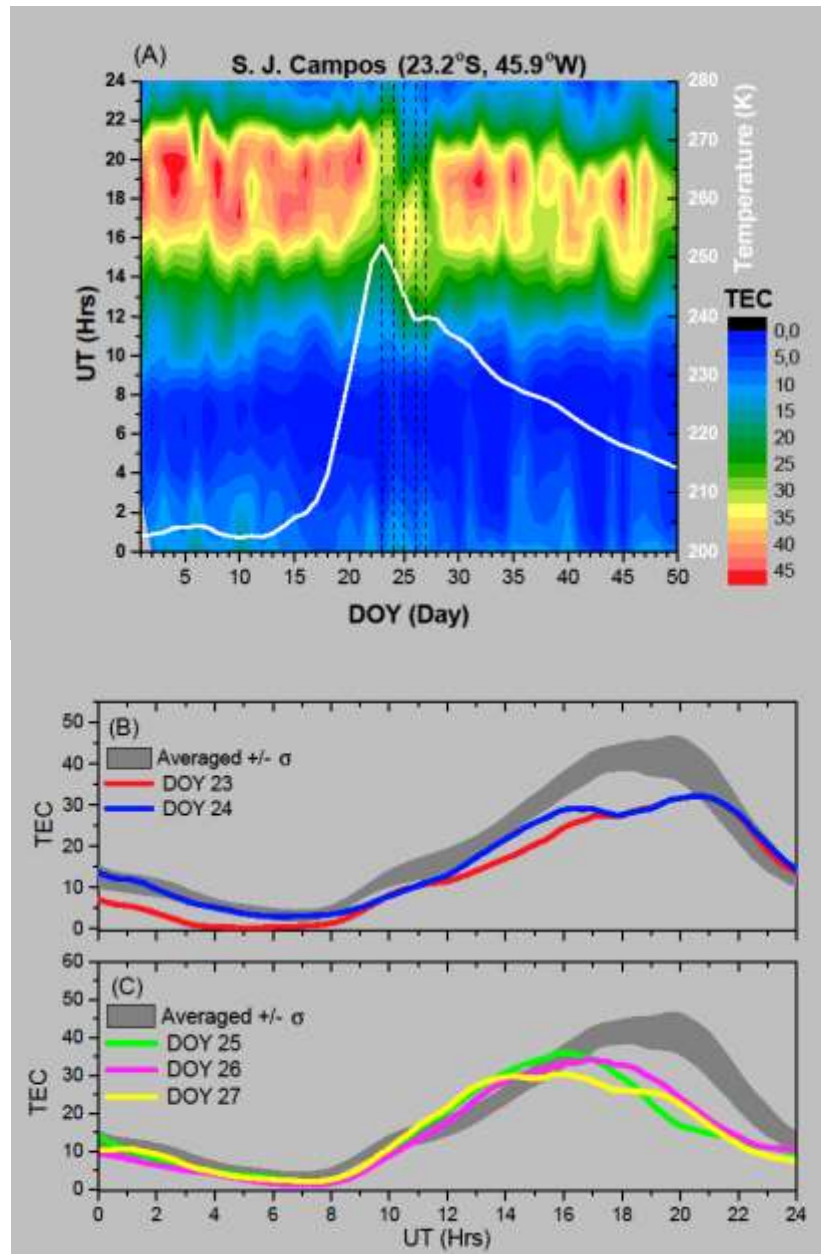
591 Figure 1- South American map showing the locations of GPS and Digital
592 Ionosonde stations. The blue and green icons indicate stations that are
593 analyzed in more details. The GPS stations along the black colored dashed
594 line are used to study the EIA characteristics during the present SSW event.



595

596 Figure 2- Plots showing the stratospheric temperatures at 90oN and 60o-90oN
597 (averaged) at 10 hPa (~30 km) in the northern hemisphere during the period
598 January-February, 2009.

599



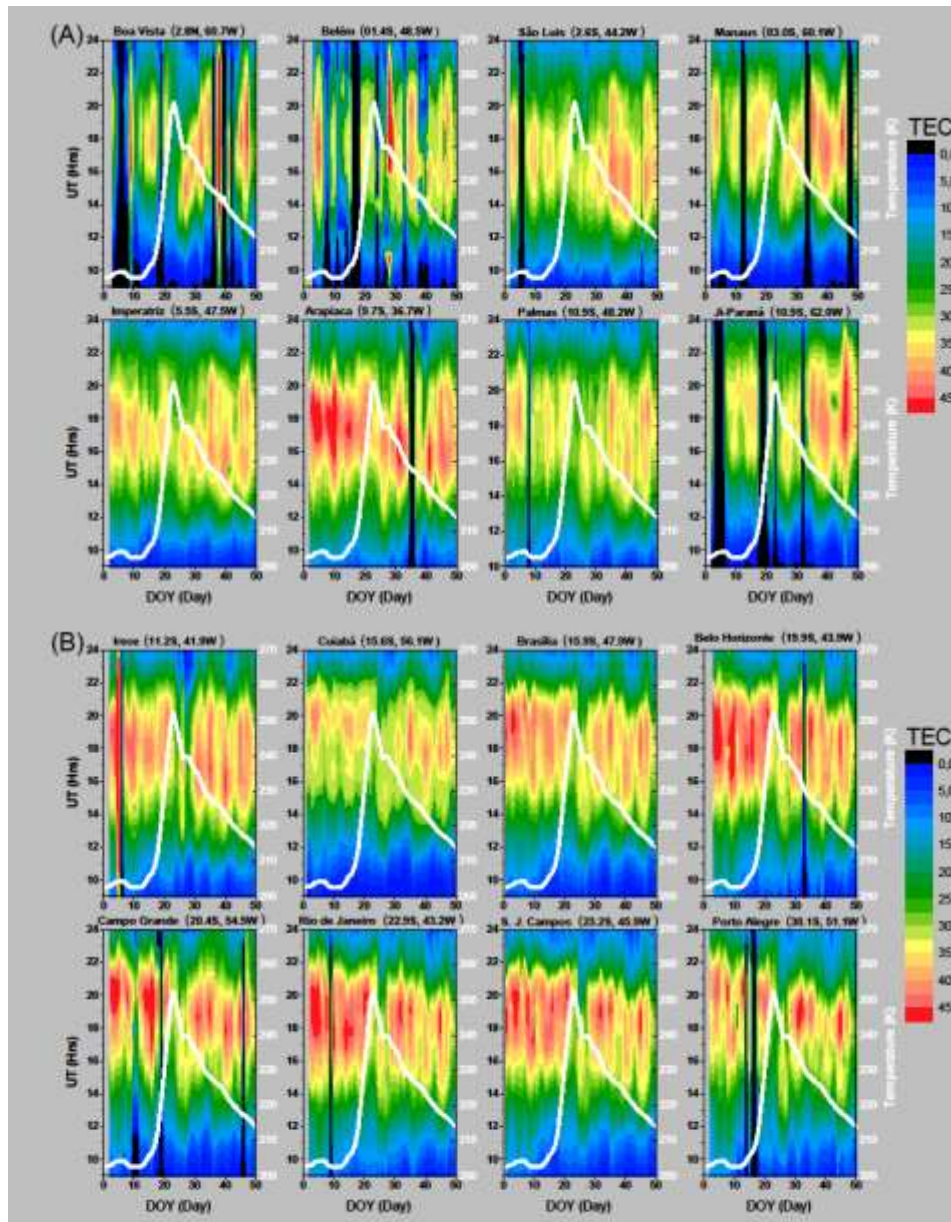
600

601

602 Figure 3- (A) Contour plot showing the VTEC variations with UT as a function of
 603 DOY (January-February, 2009) at Sao Jose dos Campos (23oS, near the EIA
 604 crest). The white solid line shows the average stratospheric temperature
 605 variations between 60oN to 90oN at 10hPa (~30km), and the dashed lines
 606 indicate the DOY from 23 to 27. (B). The VTEC diurnal variations during
 607 disturbed days (DOY 23 and 24). The averaged quiet-day VTEC is shown as

608 gray bands with the band widths indicating ± 1 standard deviation. (C) The
609 same as (B) but for DOY 25, 26, and 27.

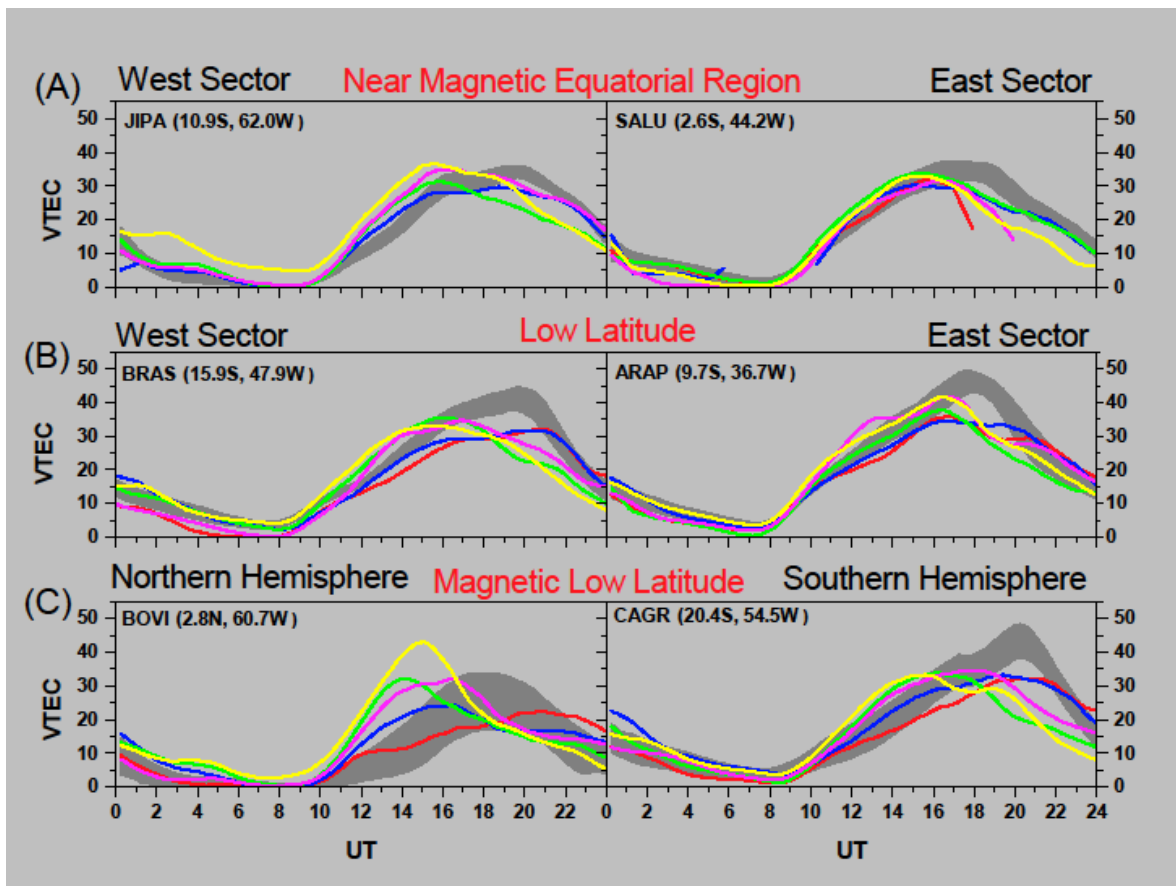
610



612

613 Figure 4- (A) VTEC variations with UT as a function of day of the year (January-
614 February, 2009) for 8 stations over Brazilian sector, spanning from latitude
615 2.8oN to 10.9oS and longitude from 36.7oW to 62.0oW. (B) VTEC variation

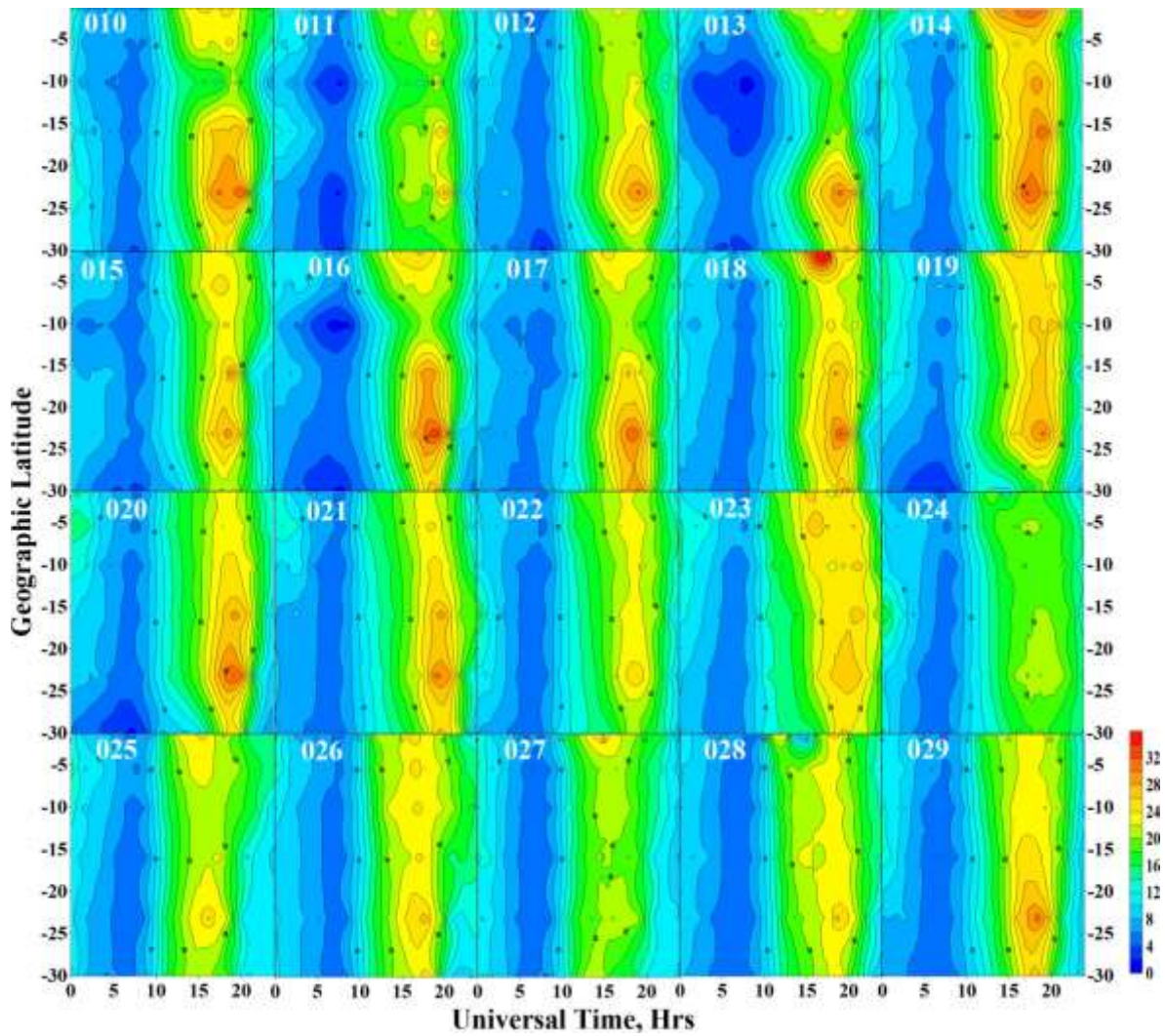
616 with UT as a function of day of the year (January-February, 2009) for 8 stations
 617 over Brazilian sector, spanning from latitude 11.2oS to 30.1oS and longitude
 618 41.9oW to 56.1oW. The white solid lines show the average stratospheric
 619 temperature variation between 60oN to 90oN at 10hPa (~30km).



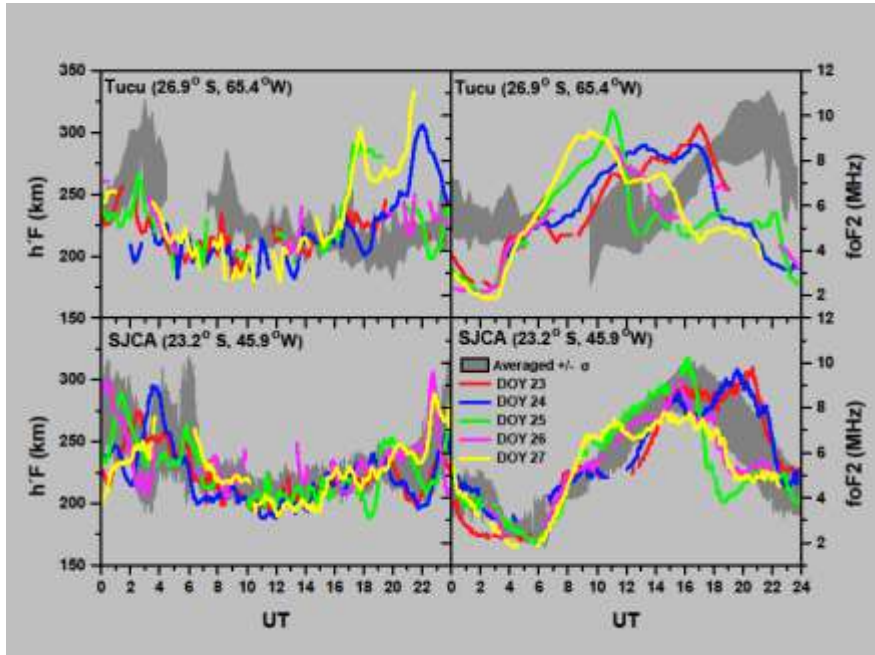
620

621 Figure 5- (A) The averaged quiet-day diurnal VTEC variations is shown as gray
 622 bands with the band widths indicating ± 1 standard deviation and the variation
 623 of VTEC during the disturbed period (DOY 23 to 27) over near magnetic
 624 equatorial region (Ji-Parana - JIPA and Sao Luis - SALU). (B) The same as (A)
 625 but for low-latitude (Brasilia - BRAS and Arapiaca - ARAP). (C) The same as

626 (A) but for Boa Vista (BOVI) located in the magnetic North Hemisphere and
627 Campo Grande (CAGR) located in the South Hemisphere.



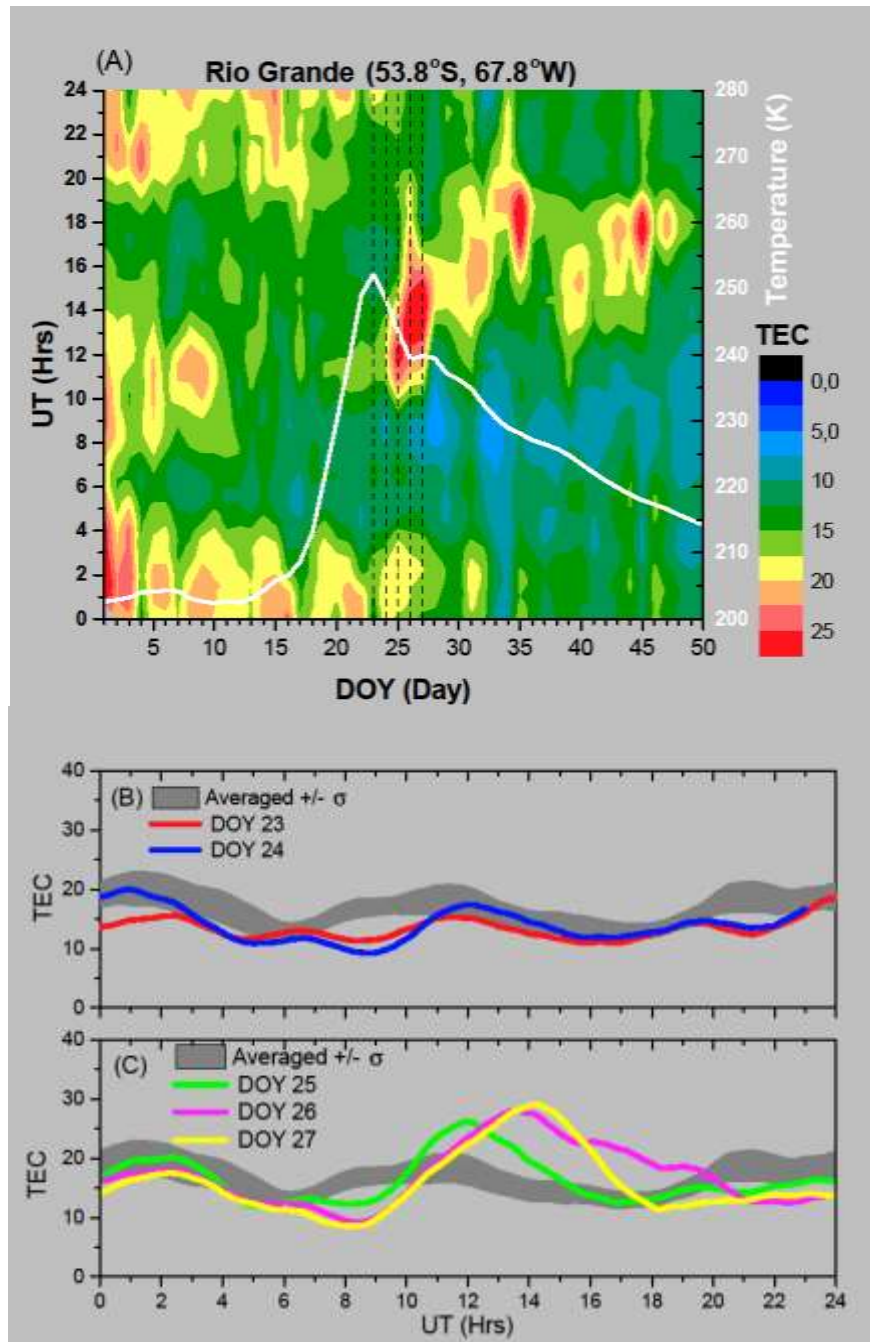
628
629 Figure 6- Contour plots showing the daily VTEC variation as a function of
630 geographic latitude and UT from DOY 10 to DOY 29. The latitude starts from
631 equator to the EIA crest in the southern hemisphere and beyond.



632

633 Figure 7- Variations of h'F and FoF2 during the period from DOY 23 to DOY 27 at
 634 Tucuman (TUCU) and Sao Jose dos Campos (SJCA). The averaged quiet-day
 635 h'F and foF2 values are shown as gray bands with the band widths indicating
 636 ± 1 standard deviation.

637



638

639

640 Figure 8- (A) VTEC variations with UT as a function of DOY (January-February,
 641 2009) at Rio Grande (53.8oS, mid-latitude), the white solid line show the
 642 average stratospheric temperature variation between 60oN to 90oN at 10hPa
 643 (~30km), and the dashed lines indicate the DOY from 23 to 27. (B) The
 644 averaged quiet-day VTEC is shown as gray bands with the band widths

645 indicating ± 1 standard deviation and the variation of VTEC during the disturbed
646 period of DOY 23 and 24. (C) The same as (B) but for DOY 25, 26, and 27.